Cement and Concrete Research 40 (2010) 1590–1600

Contents lists available at ScienceDirect

Cement and Concrete Research

journal homepage: http://ees.elsevier.com/CEMCON/default.asp

Identification of microstructural characteristics in lightweight aggregate concretes by micromechanical modelling including the interfacial transition zone (ITZ)

Y. Ke [a], S. Ortola [a,*], A.L. Beaucour [a], H. Dumontet [b,c]

[a] University of Cergy-Pontoise, Laboratoire de Mécanique & Matériaux du Génie Civil, EA 4114, F-95000 Cergy-Pontoise, France
[b] UPMC Univ Paris 06, UMR 7190, Institut Jean le Rond d'Alembert, F-75005, Paris, France
[c] CNRS, UMR 7190, Institut Jean le Rond d'Alembert, F-75005, Paris, France

ARTICLE INFO

Article history:
Received 12 October 2009
Accepted 6 July 2010

Keywords:
Lightweight aggregate concretes (LWAC)
Interfacial transition zone (ITZ)
Elastic moduli
Composite
Modelling

ABSTRACT

An approach which combines both experimental techniques and micromechanical modelling is developed in order to characterise the elastic behaviour of lightweight aggregate concretes (LWAC). More than three hundred LWAC specimens with various lightweight aggregate types (5) of several volume ratios and three different mortar matrices (normal, HP, VHP) are tested. The modelling is based on iterative homogenisation process and includes the ITZ specificities experimentally observed with scanning electron microscopy (SEM). In agreement with experimental measurements, the effects of mix design parameters as well as of the interfacial transition zone (ITZ) on concrete mechanical performances are quantitatively analysed. Confrontations with experimental results allow identifying the elastic moduli of LWA which are difficult to determine experimentally. Whereas the traditional empirical formulas are not sufficiently precise, predictions of LWAC elastic behaviours computed with the micromechanical models appear in good agreement with experimental measurements.

1. Introduction

In recent years, with the development of high performance concrete technology, the lightweight aggregate concrete (LWAC) has regained significant interest because of its advantages as low weight, improved thermal and acoustic insulations and better resistance to frost and fire. LWAC finds several applications [1], such as high-rise building, long-span bridges [2], offshore platform [3] and thermal insulation and soundproofing of house. Manufactured lightweight aggregates (LWAs) are made from natural materials such as clay, shale, slate, vermiculite, perlite or from industrial by-products as blastefurnace slags, fly ash or expanded polystyrene. In France, the most used LWAs are artificial expanded clay or expanded shale. The elastic properties of these aggregates are difficult to measure experimentally, because mechanical tests, such as uniaxial compression or ultrasonic, need to polish the grain. Polishing removes the outer shell of the grain and leads to a loss of the elastic properties of the lightweight aggregate. So the elastic behaviour is usually evaluated only from the dry volume density of the aggregate, but the corresponding Young's modulus is not precise enough and leads to errors on the predictions of macroscopic behaviour of concretes.

Therefore, it is interesting to improve the understanding of the different components' influence (quality, proportions) on the mechanical properties of LWACs in order to optimise their mix designs toward the density/mechanical performance ratio. A double approach is carried out by coupling experimental studies with numerical modelling. Multi-scale models are developed for LWACs according to the specificities of their microstructure experimentally observed. The interest of a combined study is to correlate the qualities and the proportions of the different constituents to the strength and the stiffness of LWACs. Furthermore, a simulation tool is useful to reduce the cost and duration of the experimental mix design studies. In addition, multi-scale modelling allows identifying microstructural characteristics of LWAC (Young's modulus of LWA, Young's modulus and thickness of the interfacial zone) difficult to measure accurately; this leads to a better precision of some intrinsic values and thus to a better prediction of the macroscopic behaviours observed during experiments. We use in this work iterative homogenisation [1,4]. Homogenisation methods have been widely used to predict the behaviour of many composite materials [5–7] and in particular that of concretes [8–10]. They also have been used to determine, by inverse approach, the local behaviours of the phases [11,12]. Although many references are available on cementitious materials [13,14], lightweight aggregate concretes have been less studied by these approaches. The homogenisation techniques consist in defining the equivalent homogeneous behaviour of concretes from the characteristics of the mortar matrix, the aggregates and the ITZ, and from their respective proportions. Homogenisation models then need to know the characteristics of the microstructure and are sensitive to the rate of reinforcement and to the differences in the phases' behaviours.

Three types of expanded clay aggregates, two types of expanded shale aggregates and three different mortar matrices, normal, high

* Corresponding author. Tel.: +33 1 34 25 69 11; fax: +33 1 34 25 69 41.
E-mail address: sophie.ortola@u-cergy.fr (S. Ortola).

0008-8846/$ – see front matter © 2010 Elsevier Ltd. All rights reserved.
doi:10.1016/j.cemconres.2010.07.001

Table 1
Mix proportions of the lightweight aggregate concretes 4/10 550 A.

	W/b	W (kg/m^3)	C (kg/m^3)	SF (kg/m^3)	S (kg/m^3)	SP (kg/m^3)	LWA (ssd) (kg/m^3)	V_a
M8	0.446	336.24	753.9	–	1055.46	–	0.00	0
		294.21	659.66	–	923.53	–	142.20	0.125
		252.18	565.42	–	791.59	–	284.40	0.25
		210.15	471.19	–	659.66	–	426.60	0.375
		184.93	414.64	–	580.5	–	511.92	0.45
M9	0.35	283.98	811.38	–	1135.94	8.11	0.00	0
		248.49	709.96	–	993.95	7.10	142.20	0.125
		212.99	608.54	–	851.95	6.09	284.40	0.25
		177.49	507.11	–	709.96	5.07	426.60	0.375
		156.19	446.26	–	624.77	4.46	511.92	0.45
M10	0.29	263.64	826.45	82.64	1074.38	19.83	0.00	0
		230.68	723.14	72.31	940.08	17.36	142.20	0.125
		197.73	619.83	61.98	805.79	14.88	284.40	0.25
		164.77	516.53	51.65	671.49	12.4	426.60	0.375
		145	454.55	45.45	590.91	10.91	511.92	0.45

b: binder, ssd: saturated-surface-dried.

performance (HP) and very high performance (VHP), were used for the realization of the concrete specimens. The elastic characteristics of the constituents, measured for all the studied concretes, are presented in the first part. An example of mix design is specified. The measured macroscopic elastic behaviours are, in second part, compared with the predictions obtained by some classical homogenisation models based on two-component schemes [15,16]. Different explicit models of the literature are implemented [17–20]. Their application to the prediction of LWAC behaviours shows a wide disparity between the different approaches, especially when the volume fraction of reinforcement is greater than 40% and when the contrast between the phases grows. In order to extend the range of validity for the prediction of LWAC's behaviours, an iterative procedure is coupled with the classical homogenisation models [1,4]. The resulting improved numerical tool leads to a unique prediction of the effective behaviours of LWAC and its efficiency is exposed. Iterative homogenisation is moreover used to identify, by inverse approach, the Young's moduli of the lightweight aggregates in order to introduce more precise parameters in the modelling. The correction issued from identifications based on a two-component model is discussed [21]. It seems essential to introduce the interfacial transition zone (ITZ) into the chosen modelling in order to predict the experimental LWACs behaviours, as well as to develop identification procedures of microstructural properties. Interfacial transition behaviour can be introduced by asymptotic methods [22] (interface with no thickness), or three-phase modelling [12,23] or numerical procedure of finite element with material discontinuity [24]. The characterization of the interphase zone between aggregate and cement paste in LWACs is studied with scanning electron microscopy (SEM) observations and presented in the third part. According to these experimental observations, the improvement of the micromechanical modelling and the identification strategy are exposed in the fourth and last parts. The improved iterative homogenisation based on a three-component scheme is used to identify microstructural characteristics in LWACs, as LWA and ITZ characteristics. The contributions of the three-component iterative scheme and of the microstructural identifications are finally exposed and discussed through their confrontations with experimental results.

2. The lightweight aggregates and concretes tested in experiments

In the experimental study, five LWAs are used: three expanded clay aggregates (A) of quasi-spherical shape (0/4 650 A, 4/10 550 A, 4/10 430 A) and two aggregates of expanded shale (S) of irregular shape (4/10 520 S, 4/8 750 S). The three used matrices (called M8, M9 and M10) are made of Portland cement mortar CEM I 52.5 and normal sand 0/2 mm. Series of cylindrical specimens ϕ 16×32 cm are made with a similar matrix, but different lightweight aggregates. The volume fraction of the aggregates (c_a) varies from 0.125 to 0.45 and the corresponding concretes are noted $C_{0.125}$, $C_{0.25}$, $C_{0.375}$, and $C_{0.45}$ so that C_0 designs the mortar matrix. Details of the mix proportions and experimental procedure are available in reference [25]. Samples are cured in water during 27 days and uniaxial compression tests are carried out on all specimens at 28 days. Samples undergo three loading–unloading cycles from 0.5 MPa to the third of the ultimate load, according to the recommendations of LCPC [26]. The Young's moduli (of mortar and LWAC) are determined from the slopes of the second and third loading cycles. All tested formulations and experimental results are available in [1]. The following paragraphs indicate some details about the mixture proportions, the characteristics of lightweight aggregates and the measured elastic behaviours of LWAC.

2.1. Presentation of components and mixture proportions

In all the mixture proportions, the W/C or W/(C + SF) ratios and the S/C ratio remain constant (Table 1) for all the concretes made of a given matrix (W: water; C: cement; S: sand; SF: silica fume). The S/C ratio is equal to 1.4. The proportions of superplasticizers added to M9 and M10 matrices are adapted in order to ensure the same slump for all the families of LWACs. For M10 matrix, the silica fume added in the formulation represents 10% of the used cement mass. For example, mixture proportions of LWAC made of 4/10 550 A aggregates are reported in Table 1.

The Young's modulus of the three mortar matrices are experimentally identified to 28.6 GPa for M8, 33.2 GPa for M9 and 35.4 GPa for M10 (Table 3). Their measured compressive strength values are 40 MPa, 64 MPa and 86 MPa respectively [27], so that they correspond to a matrix called normal, high performance (HP) and very high performance (VHP).

2.2. Experimental results

On the whole, 63 formulations (more than 300 specimens) of LWACs have been studied during experiments and extended results are available in [1]. Usually, the Young's modulus of aggregates is estimated by using empirical relations with the particle dry density of LWAs ρ_a. Lower and upper bounds have been established from experimental measures [28] and the mean value between these bounds gives the following equation (Eq. (1)) to estimate the Young's modulus of LWA E_a:

$$E_a = 8000 \times \rho_a^2 \quad (1)$$

The dry densities of the studied clay and shale aggregates are presented in Table 2 and the values of bounds and mean (Eq. (1)) are also reported.

Table 2
Physical and mechanical properties of LWAs.

LWA	0/4 650 A	4/10 550 A	4/10 430 A	4/10 520 S	4/8 750 S
Particle dry density ρ_a (kg/m^3)	927	921	737	901	1577
External shell thickness e (mm) [25]	–	0.12	0.22	0.23	0.10
Empirical bounds E_a (MPa) [28]	6000–9400	5900–9300	4000–6250	5700–9000	16,300–not quoted
Mean empirical value E_a (MPa)	6870	6790	4340	6490	19,900

Uniaxial compression tests are carried out on all specimens in order to determine the Young's moduli of mortar and LWACs. The characterization of all the LWAC Young's moduli allows studying their sensibility to the various types of aggregates and to their respective volume fractions. Three specimens are manufactured and tested for each C_j material. Table 3 gives the corresponding average values.

As the volume fraction of aggregates increases, the Young's modulus of concretes goes down from 28,600 MPa to 15,700 MPa with the ordinary matrix M8, from 33,200 MPa to 17,200 MPa with the HP matrix M9, and from 35,400 MPa to 20,100 MPa with the VHP matrix M10. For a given percentage of aggregates, the 4/8 750 S concretes have the greater elastic modulus, whatever the mortar matrix. The concrete with aggregates 0/4 650 A presents the lowest Young's modulus with the matrix M8. However, with the increase of the matrix rigidity (M9 then M10), the weakest Young's modulus is obtained for the 4/10 430 A aggregate concretes. These measurements are used in the following to study the accuracy of some classical homogenisation models with respect to the specificities of LWAC elastic behaviours.

3. Analysis of experimental results with several homogenisation schemes

In mechanics of materials, the procedure of homogenisation replaces a heterogeneous material by an equivalent homogeneous material that responds in the same way to a macroscopic loading. An equivalent behaviour law is written at a macroscopic scale, based on the behaviour laws, at a microscopic scale, of the various phases of the studied heterogeneous material. For concretes, the microscopic level can be the scale at which the mortar matrix distinguishes from aggregates, while the macroscopic scale at which the concrete can be considered as homogeneous, can be the scale of the structures (concrete beam or column).

For fifty years, many homogenisation methods have been proposed and the literature is consistent [29–31]. General developments on heterogeneous materials can be found in standard references like [6,7,15,32,33]. Some manuscripts, such as [9,34–37], treat more specifically of periodic homogenisation. [38,39] refer to the morphological approach. Specific references to cementitious materials are available in [10,12,40,41]. More recently, a large number of authors have proposed multi-scale developments on transfers in heterogeneous porous media [42–44]. We compare in the following the predictions of some classical homogenisation schemes with the elastic moduli of the concretes measured in experiments (Table 3). We then proposed to reduce the observed differences by using iterative homogenisation [21] and by improving the estimations of the Young's modulus of the lightweight aggregates (Table 2).

Table 3
Experimental Young's modulus of the various LWACs.

E_c (MPa)		C_0	$C_{0.125}$	$C_{0.25}$	$C_{0.375}$	$C_{0.45}$
M8	0/4 650 A	28,588	23,539	20,665	16,743	15,669
	4/10 550 A		26,157	21,680	17,900	16,606
	4/10 430 A		24,900	21,391	17,293	15,699
	4/10 520 S		25,135	22,471	19,428	18,286
	4/8 750 S		27,367	26,262	25,281	24,324
M9	0/4 650 A	33,183	29,396	23,712	19,871	17,175
	4/10 550 A		29,159	24,934	21,358	19,696
	4/10 430 A		27,568	23,778	20,818	18,935
	4/10 520 S		29,480	26,521	22,188	20,184
	4/8 750 S		31,931	30,987	30,146	29,311
M10	0/4 650 A	35,397	31,147	26,753	22,427	20,346
	4/10 550 A		32,089	27,991	23,684	21,724
	4/10 430 A		30,220	26,033	22,296	20,082
	4/10 520 S		32,783	27,998	24,340	22,024
	4/8 750 S		34,213	33,845	32,945	33,002

3.1. Homogenisation of Young's moduli of LWACs using classical homogenization methods

The LWACs are considered, in this section, to be made of only two linear elastic phases (matrix and aggregate). The selected homogenisation schemes are: the optimal bounds of Hashin–Shtrikman [45], the Mori–Tanaka scheme [19,20] and the approximation of De Larrard and Le Roy [46]. The homogenisation approach proposed by Hashin and Shtrikman [45] is an energy approach which provides the optimal upper (HS-max) and lower (HS-min) bounds of the equivalent behaviour of an elastic two-phase composite. The Mori–Tanaka scheme allows taking into account the interaction between the inclusions as their volume fraction in the heterogeneous material increases. For this purpose, this scheme approximates the average strain in the reinforcement by the average strain of a single inclusion in an infinite matrix subjected to the uniform average strain of the matrix. From Hashin's model of the concentric spheres [18], De Larrard and Le Roy [46] proposed a modelling (DLR) to take into account the size distribution of the granular skeleton. Other historical schemes, like the bounds of Voigt and Reuss [32], as well as their different combinations are available in [1,21].

The predictions of the LWAC Young's modulus E_c are confronted with our experimental results (Table 3) in Fig. 1. The elastic behaviours of the components result from Table 3 for the mortar matrices and from Table 2 for the average values of the Young's modulus of aggregates E_a estimated by the empirical relation (Eq. (1)). As expected, the predictions of the Mori–Tanaka scheme (MT) and the Hashin–Shtrikman upper bound (HS-max) are similar, as the matrix Young's modulus E_m is superior to the aggregate's one E_a. Both predictions slightly underestimate the experimental LWAC Young's modulus E_c, whereas the Hashin–Shtrikman lower bound (HS-min) remains away from the measured experimental values. The (DLR) approach remains distant from the experimental values.

The differences between the various predictive models and the experimental measurements have been also computed according to the moduli ratio E_a/E_m of the phases and to the proportion of reinforcements c_a in LWACs [1]. The corresponding errors present similar tendencies: when the contrast of rigidity grows between the two phases, the errors increase for all the models and the most accurate predictions are given by the Hashin–Shtrikman upper bound (HS-max) and the Mori–Tanaka approach (MT). The errors between the homogenisation models and the experimental results increase with the volume fraction of aggregates c_a in all LWACs.

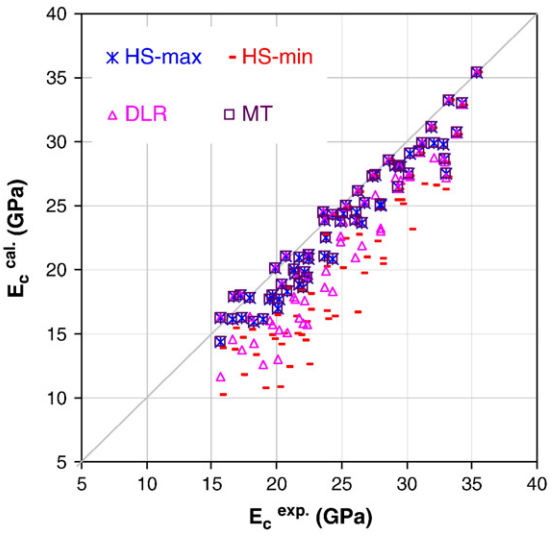

Fig. 1. Confrontation of LWACs Young's modulus between our experimental results (Table 3) and the predictions of some classical homogenisation models.

Overall, the models underestimate the measured elastic properties independently of the aggregate/mortar elastic moduli ratio and whatever the proportion of aggregates in the formulations. In particular, the predictions show a wide disparity when the volume fraction of reinforcements exceeds 40% and when contrast between the phases grows. These parameter ranges correspond exactly to the characteristic values of concrete mixes, and it thus appears necessary to develop predictive methods more adapted to the specificities of LWACs. The choices for improvement focused on two points: the implementation of a homogenisation method independent of mixture characteristic (E_a/E_m ratios and volume fractions c_a) and the use of corrected microstructural data (E_a).

3.2. Iterative homogenisation

The principle of iterative homogenisation is to gradually homogenise the behaviour of heterogeneous materials by introducing n virtual intermediate materials by adding a small fraction of reinforcement to the previous step [4,21]. Iterative homogenisations have been studied for ten years now, and their effectiveness has been proven and successfully used for several applications. References are available on elastic behaviour of unidirectional composites [47], syntactic foams [48], lightweight aggregate concretes [21] and polydispersed heterogeneous materials [4]. Iterative homogenisation has proved to be also adapted to predict non-linear behaviours of porous media [49]. Iterative homogenisation can be based on any localization method, regardless of the strain or stress approach. We present below the unique converged solution computed, for example, from the Dilute Approximation, the Mori–Tanaka scheme and the Hashin–Shtrikman upper bound. Other iterative schemes can be found in [1,4].

Fig. 2 shows that predictions become unique (continuous line), whatever the used homogenisation scheme (dotted lines), and whatever the type of LWAC. Furthermore, the unique computed prediction respects the Hashin–Shtrikman bounds [1,4]. Also, only the simplest localisation method is conserved in the following, the Dilute Approximation in strain approach (IDA), so that the corresponding numerical tool is easy and economic. It may be noted in Fig. 2 that, although the homogenisation predictions are unified, some differences remain to experimental measurements. To remove them, the iterative homogenisation is then used in the following to improve the values of the Young's modulus of LWA E_a used in the micromechanical predictions.

3.3. Identification of Young's moduli of LWAs based on iterative homogenisation and a two-phase model

Predictions of Fig. 2 have been computed with the average empirical values of E_a (Table 2). The purpose of this part is to correct these empirical values using micromechanical modelling. Indeed, the homogenisation approach allows determining some properties of the components, in particular, those difficult to measure from experiments. For example, Schmitt et al. [11] used a generalized self-consistent scheme to identify the moduli of ceramics components (alumina, mortar). Hashin and Monteiro [12] also developed an inverse methodology based on the generalized self-consistent scheme to determine microstructural elastic properties in mortars.

We here use an inverse approach based on the iterative homogenisation to determine the Young's modulus of aggregates E_a from the experimentally measured values [21]. The measured Young's modulus of concretes $E_c^{exp.}$ and mortar matrices $E_m^{exp.}$ (Table 3) are introduced in the modelling as well as the volume fraction of aggregates c_a^{exp} used in the mixes. As the Poisson's ratios of the components have a negligible influence on the equivalent Young's modulus of the concrete [1], the Poisson's ratio of the aggregates and of the mortar matrices are chosen identical and equal to 0.2. This choice is commonly adopted [12,46,50,51]. The identification procedure is initialised by the empirical value of the LWA Young's modulus (Eq. (1)). This initial value E_a (Table 2) is then used to compute, with the iterative homogenisation, the equivalent Young's modulus of concrete $E_c^{cal.}$. This calculated effective modulus is then compared to the experimentally measured one $E_c^{exp.}$. If these two values $E_c^{cal.}$ and $E_c^{exp.}$ differ, the value E_a is corrected until the new computed value $E_c^{cal.}$ leads to a relative error lower than 0.01 [21]. The identification of the Young's modulus E_a, carried out from M8 concretes, is presented in Table 4.

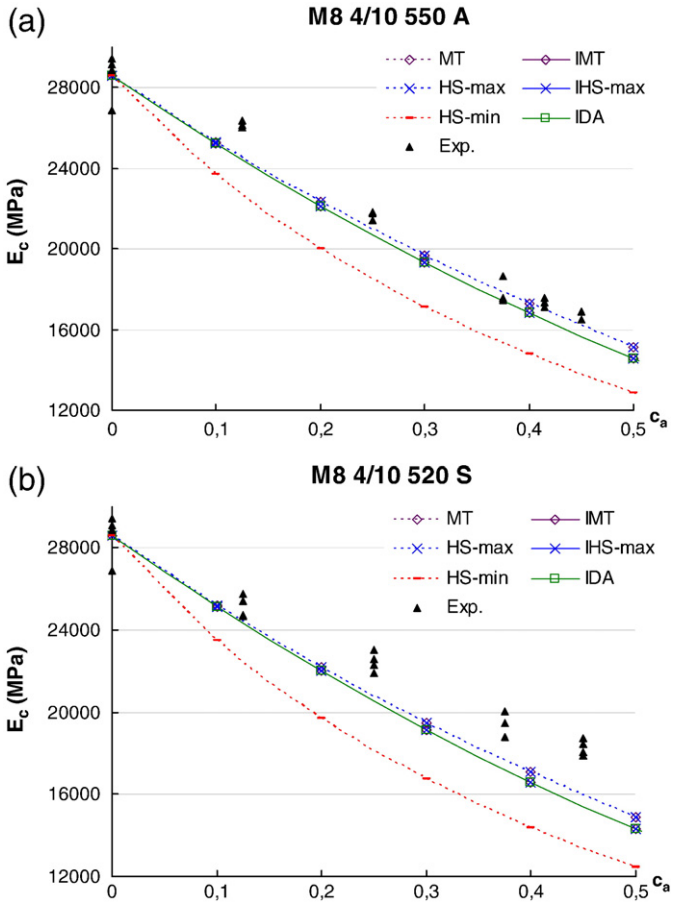

Fig. 2. Predictions computed with iterative homogenisation and comparison to the measured Young's modulus of LWACs; (a) concretes M8 4/10 550 A; (b) concretes M8 4/10 520 S.

These identified LWAs Young's moduli E_a are then used in the iterative homogenisation (IDA) for all the studied LWACs. The improvements are illustrated in Fig. 3 for one type of expanded clay LWC (concretes M8 4/10 550 A) and one of expanded shale LWC (concretes M8 4/10 520 S). For comparison, the predictions of LWAC's Young's modulus E_c by iterative homogenisation (IDA) are also plotted by using the lower ($E_{a\ \mathrm{inf}}$) and the upper ($E_{a\ \mathrm{sup}}$) bounds of the empirical estimations (Table 2).

The experimental results and the predictions of the Young's modulus E_c for the expanded clay concretes M8 4/10 550 A are between the simulations computed with the empirical bounds ($E_{a\ \mathrm{inf}}$)

Table 4
Young's modulus of LWAs E_a identified from M8 concretes [25].

LWAs	0/4 650 A	4/10 550 A	4/10 430 A	4/10 520 S	4/8 750 S
E_a identified from M8 (MPa)	6470	8030	7183	10,077	20,273

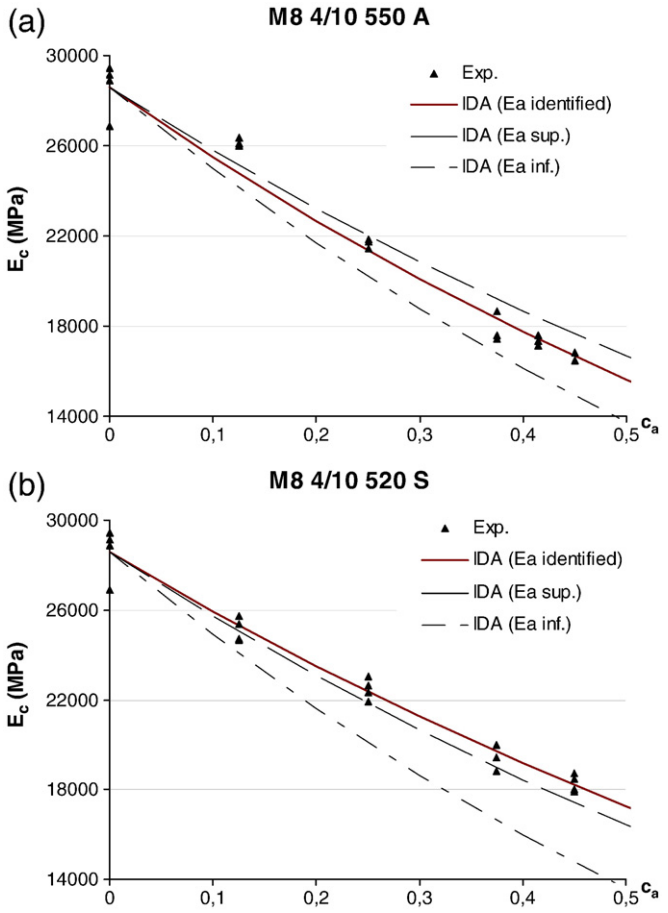

Fig. 3. Evolution of LWACs Young's modulus $E_c^{cal.}$ computed with the identified LWAs Young's modulus E_a (Table 4) and with the empirical LWAs Young's modulus bounds ($E_{a\ inf}$) and ($E_{a\ sup}$) (Table 2). Confrontations experiments/modelling: (a) concretes M8 4/10 550 A; (b) concretes M8 4/10 520 S.

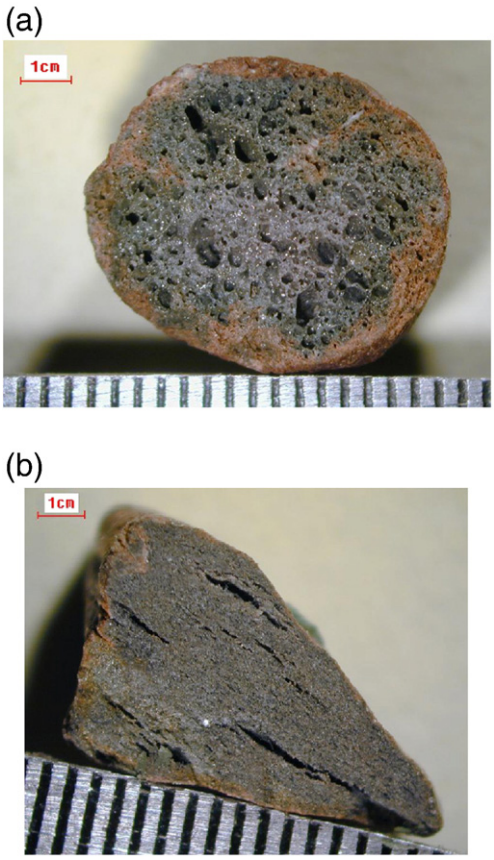

Fig. 4. Section of 4/10 430 A (a) and 4/8 750 S (b) lightweight aggregates.

and ($E_{a\ sup}$) (Fig. 3a). The other families of concretes M8 0/4 650 A and M8 4/8 750 S show a similar tendency [1].

On the other hand, experimental measurements and simulations of the Young's modulus E_c for the expanded shale concretes M8 4/10 520 S exceed the predictions corresponding to the upper empirical value ($E_{a\ sup}$) (Fig. 3b). This is due to the identified values of E_a (Table 4), which are higher than the upper empirical bound ($E_{a\ sup}$) (Table 2). Similar behaviour is also observed for concretes M8 4/10 430 A [1]. These differences may be explained by the range of uncertainty of the empirical relations and by the measurement method of E_a which requires polishing the aggregates. Indeed, empirical estimations of the LWA Young's modulus show large variations for the same aggregate's density value. Furthermore, the external stiffer dense shell is removed and the elastic modulus may be underestimated [5,52]. Thus, the underestimation is even more pronounced for aggregates 4/10 520 S and 4/10 430 A (Fig. 4a) which have an outer shell two times thicker than those of the other LWA (Table 2).

The identified Young's moduli of the aggregates 0/4 650 A and 4/8 750 S (Table 4) are quite close to the average empirical values (Table 2). This good agreement is explained by the fact that these LWAs have a homogeneous structure and do not present a denser outer shell (Fig. 4b). These remarks underline that the sample preparation before measurement changes only the mechanical properties of the aggregates having the thickest external shells. They also suggest that another way to evaluate the Young's modulus of lightweight aggregates E_a is necessary. In addition, there exist transition zones between the lightweight aggregates and the mortar matrix, whose microstructure and strength vary according to the matrix water to cement ratio and the type of aggregate.

Using an inverse approach based on a two-component homogenisation scheme in fact leads to the characteristics of the LWA coated with this interfacial zone. This remark can be illustrated with Fig. 5 which illustrates the results of the identification procedure of E_a when independently used with the experimental measures of the other series of concretes M9 and M10. The experimental results for $c_a = 12.5\%$ are not mentioned because of the segregation sometimes observed for the small percentages of aggregates, which influences the mechanical properties of concretes. If segregation occurs, concretes cannot then be considered as an equivalent homogeneous material anymore. The experimental measures of their Young's modulus E_c are no more representative and the corresponding identification for the Young's modulus of the aggregates E_a is no

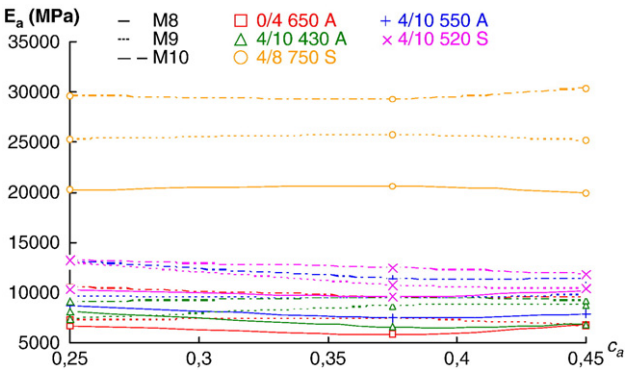

Fig. 5. Identified LWAs Young's modulus E_a from the experimental data of concretes M8, M9 and M10 (iterative homogenisation with two components).

more valid. The average values show that an identification based on a two-component modelling leads to LWA Young's modulus E_a, whose values fluctuate with the rigidity of the mortar matrix. These variations illustrate the influence of the E/C mortar ratio and point up that the transition zone between lightweight aggregate and mortar matrix cannot be neglected in the modelling [12,24]. But its effects vary with the quality of the mortar matrix and of the type of lightweight aggregate. We thus improve the predictive model and the associated inverse identification's procedure by enriching them with a new added phase (interphase zone). This third phase (3) represents the ITZ between the matrix (1) and the inclusions (2). It allows, according to the families of lightweight aggregates (type, size) and the nature of the matrix (normal, HP, VHP) simulating either the transition zone observed in concretes [12] or the impregnation of the LWA's surface by the cement paste [53,54]. These specificities of the interfacial transition zones, according to the families of LWAC, have been characterised experimentally by SEM observations, presented in the following section.

4. Analysis of the interfacial transition zone ITZ

In some lightweight concretes (LWC), specific properties of the interphases matrix/aggregate have been pointed out [53,54]. However, the references on the interphase area in LWAC lead to very different conclusions, and sometimes even opposite. Therefore, this first SEM observations study aims to know, whether or not there is an ITZ in the studied LWACs. The focus is only qualitative in order to discuss the influence of the matrix formulation with respect to the aggregate type. Indeed, the paste-aggregate bonding is dependent on the nature of the external shell of the lightweight aggregate. For the same grain, the external shell thickness can vary along its periphery and there are also variations from one grain to another. So, for each LWAC sample, the ITZ are observed and measured, by image analysis with Visilog software, around 3 different grains. The SEM study has been performed for M8 and M10 concretes (Figs. 6 and 8).

Table 5
SEM observation results for the interfacial zones in the studied LWACs.

	0/4 650 A	4/10 550 A	4/10 430 A	4/10 520 S	4/8 750 S
M8	Impregnation	Impregnation	ITZ (40 μm)	ITZ (20 μm)	ITZ (100 μm)
M10	Impregnation	Impregnation	No ITZ	No ITZ	No ITZ

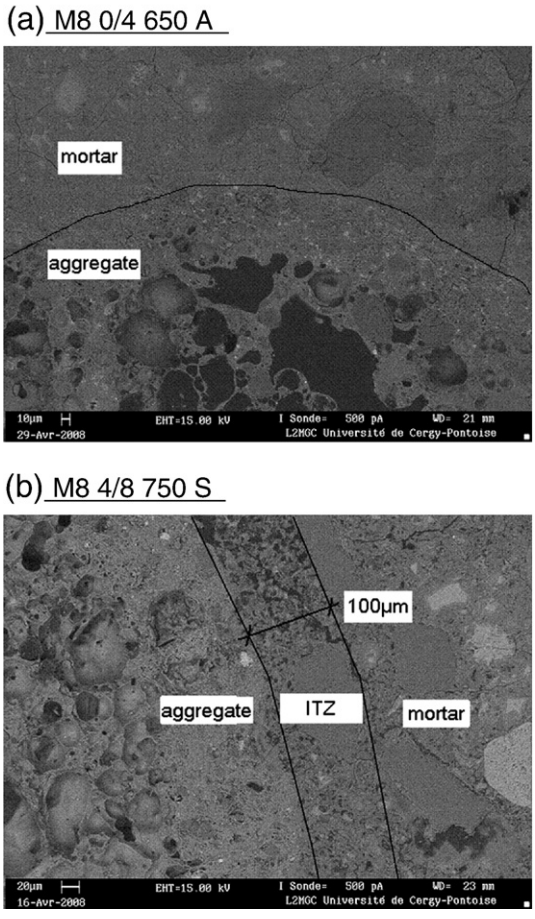

Fig. 6. Observation of mortar/aggregate interface by SEM for M8 concretes.

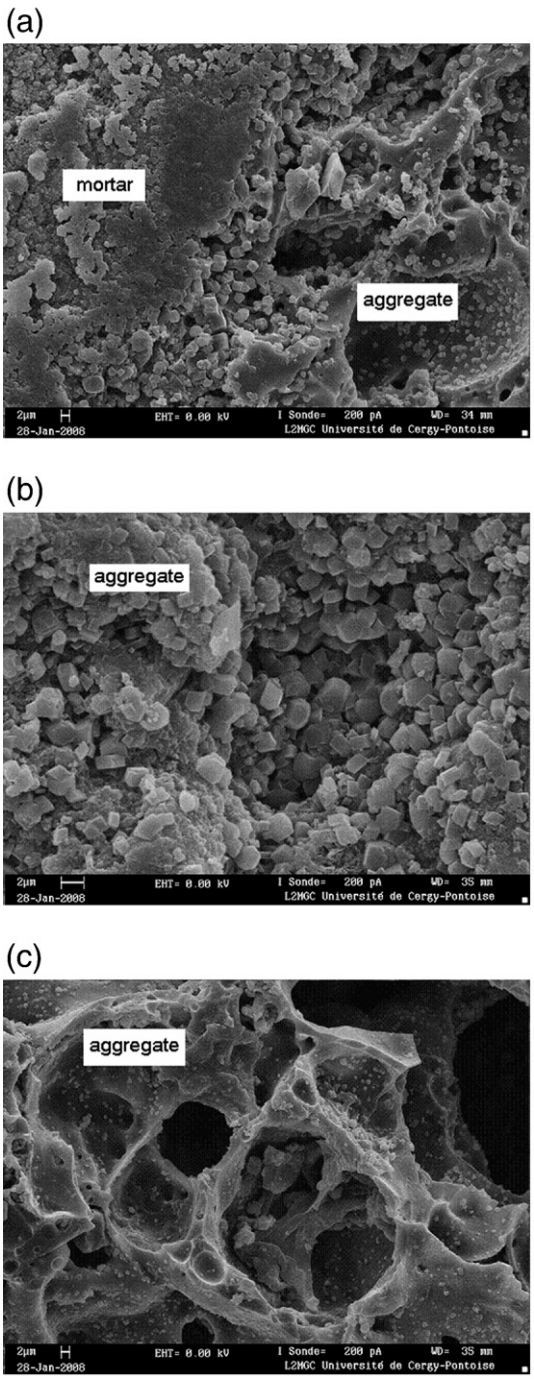

Fig. 7. Impregnation of the cement paste in aggregate 0/4 650 A. (a) Matrix/aggregate interface; (b) periphery of the grain; (c) middle of the grain.

For M8 concretes with W/C ratio equal to 0.446, a transition zone more porous than the rest of the mortar matrix is observed in the case of LWA 4/10 430 A, 4/10 520 S and 4/8 750 S (Fig. 6b): measured interphase's widths are 40 μm, 20 μm and 100 μm respectively (Table 5). However, no porous interfacial zone is observed for concretes M8 0/4 650 A (Fig. 6a). SEM images reveal white spots in the shell of the grain corresponding to anhydrous cement grains. In concretes M8 0/4 650 A (Fig. 7), the comparison between the periphery and the middle of the grain shows a filling of the pores in the grain's shell by the paste, whereas the rest of the grain retains its original microstructure. This impregnation phenomenon is also observed for the aggregates 4/10 550 A, of the same origin and of the same absorption capacity as the 0/4 650 A. Several authors have reached similar conclusions for aggregates immersed during 24 h before mixing [53–55].

The observation of the interfacial zones in M10 concretes (Fig. 8) shows reduction, or even the disappearance of the porous interfacial zone previously observed in the M8 series. The lowest W/C ratio and the presence of silica fume in these concretes lead to a reduction of the ITZ width between the LWA and the paste. For the aggregates having a high absorption capacity (0/4 650 A and 4/10 550 A), the impregnation phenomenon of the paste into the pores of surface of the aggregates is still observed.

In conclusion, the differences observed in all the interfacial zones may be related to the different absorption capacities of the LWA. The SEM observations show that there may be a transition zone between the mortar matrix and some LWA families (4/10 430 A, 4/10 520 S and 4/8 750 S). When this zone is present, its thickness e is lower and its mechanical properties are higher than those observed in normal weight concretes (NWC) (Table 6). These differences are due to the nature of the aggregates [18,50,53,54].

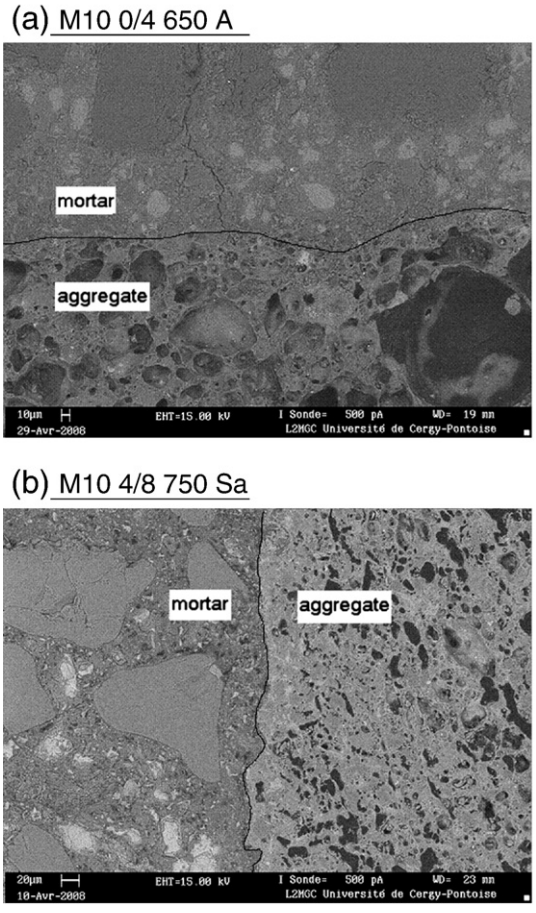

Fig. 8. SEM observation of the mortar/aggregate interface in M10 concretes.

Table 6
ITZ properties in LWAC and NWC mentioned by references.

Characteristics of the ITZ				
	LWAC		NWC	
ITZ thickness (e)	5–60 μm	[53,54]	50–100 μm	[53,54]
E_i / E_m	1/2–1	[12,50]	1/6–1	[12,50]

The observed ITZ characteristics (Table 5) will be subsequently used in the iterative homogenisation based on a three-component scheme in order to simulate the effects of the ITZ on the LWAC's macroscopic behaviours. The corresponding modelling will be noted in the following Aureole Model.

On the other hand, because of the high absorption capacity of some LWAs (0/4 650 A and 4/10 550 A), the cement paste can partially impregnate the surface of aggregates whose mechanical properties are also enhanced [54]. The improvement depends on the water to cement ratio W/C and is therefore different according to the studied matrices. The interphase in the enriched modelling can also simulate this phenomenon of the mortar impregnation on a thickness e of the LWAs. This model will be called the Impregnation Model.

According to the quantitative experimental analysis of Elsharief et al. [55], there may be an intermediate zone between the mortar and the aggregates where, because of the absorption of mixing water by LWAs, the W/C ratio is lower than that of the mortar. The mechanical properties of this intermediate zone should thus be better than those of the mortar matrix. However, this type of modelling is not suitable for the LWACs studied in this work [1].

The following section presents the enrichment of the iterative homogenisation (IDA) in order to include the interfacial transition zones (of various natures) and their influence on the macroscopic behaviours of LWACs.

5. Enriched micromechanical models for the identification of LWA and ITZ characteristics

5.1. Iterative dilute approximation with three constituents

The initial bi-phased modelling (Section 3) is enriched by introducing a new third phase between the matrix and the inclusions. So the heterogeneous material is composed of three distinct phases: an aggregate (or inclusion — phase 2) surrounded by an interphase (phase 3), both being embedded in an infinite medium (mortar or matrix — phase 1). These phases are supposed to be perfectly bonded and each one of them presents a linear elastic isotropic behaviour. In Fig. 9, a indicates the radius of the inclusion, e the thickness of the interphase (3) and b the outer radius of the inclusion surrounded by the interphase. The three-phase scheme allows simulating the various properties mentioned on the interfacial zone, according to the experimental SEM observations (Table 5) or to the reported bibliography (Table 6).

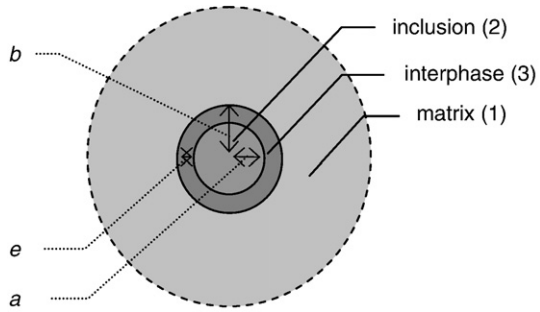

Fig. 9. The ITZ scheme model.

The equivalent rigidity tensor C_{eq} [32,33,56] is defined by:

$$C_{eq} = C_1 + c_2(C_2-C_1) : \overline{A}_2 + c_3(C_3-C_1) : \overline{A}_3 \quad (2)$$

where $\overline{A}_2$ and $\overline{A}_3$ represent the average of the localization tensors A_2 and A_3 in the phases 2 and 3 respectively. c_1, c_2 and c_3 are the respective volume fractions of the phases 1, 2 and 3, with $c_1+c_2+c_3=1$. The averages of local strains in heterogeneities check: $\overline{\varepsilon}_2 = \overline{A}_2 : E$ and $\overline{\varepsilon}_3 = \overline{A}_3 : E$ where $\boldsymbol{E}$ designs the imposed macroscopic loading in the strain approach [7,56,57].

At step j of the incremental procedure, the components of the virtual intermediate composite are the matrix (corresponding to the virtual auxiliary composite at the previous step $j-1$) and the proportions f_k of added heterogeneities (k: number of the phase), such as:

$$C_{eq}(j) = C_{eq}(j-1) + f_2(j)[C_2-C_{eq}(j-1)] : \overline{A}_2(j) + f_3(j)[C_3-C_{eq}(j-1)] : \overline{A}_3(j) \quad (3)$$

The concentration f_k verifies: $f_k(j) = \frac{\Delta c_k}{c_1 + j \times (\Delta c_2 + \Delta c_3)}$ where Δc_k represents the fraction of reinforcements added at each fictitious intermediate step when the final actual rate c_k is divided into n identical steps ($n \times \Delta c_k = c_k$) [1]. The average of the localization tensors $\overline{A}_2(j)$ and $\overline{A}_3(j)$ are the unknowns to be determined by the resolution of a cellular problem [5]. For a given macroscopic spherical loading $\boldsymbol{E}$, the trace of Eq. (3) gives the equivalent modulus of compressibility K_{eq} of the studied heterogeneous material [1]. As for example, when the iterative homogenisation is based on the Dilute Approximation (IDA) with three components, an imposed hydrostatic strain tensor $\boldsymbol{E}$ leads to localization tensors $\overline{A}_2(j)$ and $\overline{A}_3(j)$, whose traces check:

$$\overline{A}_2(j) = \frac{(b/a)^3[3K_{eq}^{IDA3}(j-1) + 4\mu_{eq}^{IDA3}(j-1)]\cdot(3K_3 + 4\mu_3)}{-12(K_2-K_3)\cdot[\mu_{eq}^{IDA3}(j-1)-\mu_3] + (b/a)^3[3K_3 + 4\mu_{eq}^{IDA3}(j-1)]\cdot(3K_2 + 4\mu_3)}$$

$$\overline{A}_3(j) = \frac{(3K_2 + 4\mu_3)}{(3K_3 + 4\mu_3)}\overline{A}_2(j) \quad (4)$$

An imposed macroscopic shear loading $\boldsymbol{E}$ leads to the equivalent shear modulus μ_{eq} of the composite material [58]. The homogenisation procedure is carried out by working with the deviator tensors and the localization tensors $\overline{A}_2$ and $\overline{A}_3$ own complex form, so they are not presented here. Further details are available in [1]. The two equivalent modulus K_{eq} and μ_{eq} allow deducing, from the classical isotropy relations, the engineer coefficients, namely the equivalent Young's modulus E_{eq} and the equivalent Poisson's ratio ν_{eq}:

$$E_{eq} = 9K_{eq}\frac{\mu_{eq}}{\mu_{eq} + 3K_{eq}} \quad \text{and} \quad \nu_{eq} = \frac{3K_{eq}-2\mu_{eq}}{6K_{eq} + 2\mu_{eq}} \quad (5)$$

Four implementations of the iterative homogenisation have been studied as well as their convergence speed [1]. Compared to reference values, iterative homogenisation proves to be an efficient numerical tool, economic, relatively flexible and easily exportable.

5.2. Identification procedure using the three-component models

Iterative homogenisation accurately predicts, as a unique converged solution, the effective behaviours whatever the volume fraction of inclusions c_2 and whatever the Young's moduli ratio E_2/E_1 of the constituents [1,21]. These advantages are particularly interesting to study the LWACs as the usual aggregate's proportions in concretes are above 40% and as the disparities between the elastic behaviours of the constituents are important ($E_a \ll E_m$). The three-component model (Section 5.1) is applied to the 15 studied families of LWAC in order to identify some microstructural properties, especially related to the LWA and the ITZ. Two procedures are exposed, according to the SEM observations (Section 4) and the literature: an Aureole Model for concretes owning a weaker and more porous zone between aggregates and mortar and an Impregnation Model for LWACs showing mortars impregnation in the periphery of the lightweight aggregates.

To the five parameters of the two-component scheme (Young's moduli E_1, E_2, Poisson's ratio ν_1, ν_2 and volume fraction c_2) are added the four parameters of the introduced model of interface with thickness (Section 5.1): the elastic moduli of the interphase (E_i, ν_i), its internal radius a and its thickness e (Fig. 9). The parameters E_1 and c_2 correspond respectively to the experimental values of the Young's modulus of the mortar matrix $E_m^{exp.}$ and to the volume fraction of aggregates $c_a^{exp.}$ contained in the mixes. The Poisson's ratio of the interphase ν_i is still supposed to be equal to 0.2, according to the usual assumptions made in the bibliography: $\nu_m = \nu_a = \nu_i = 0.2$, [12,21,46,50,51]. The average radius of the aggregate is determined from the grading curves, by the grain size at 50% sieve passing [25]. In the Aureole Model, this radius is taken equal to a; the interphase Young's modulus E_i is defined as a proportion of the mortar matrix Young's modulus $E_m^{exp.}$, according to the ratios available in the literature; the thickness e of the interphase corresponds to the measured values referred in Table 5. In the Impregnation Model, the average radius experimentally measured gives the value $b=a+e$ (Fig. 9); the Young's modulus E_i is taken equal to $E_m^{exp.}$ as the mortar matrix has impregnated the periphery of the grain; the thickness e of this impregnation zone depends on the quality of the mortar matrix (Table 8).

The adopted inverse approach is similar to that one implemented with the two-component scheme [21] and exposed in Section 3.3. It here includes the third intermediate phase in the identification of the LWA's elastic behaviours, which thus depends on five factors:

$$E_a = f\left(E_c^{exp.}, E_m^{exp.}, c_a^{exp.}, E_i / E_m^{exp.}, e / a\right) \quad (6)$$

where $E_c^{exp.}$ denotes the Young's modulus of concretes measured in experiments. The results of these identification procedures according to the different families of LWACs are presented below.

5.3. Identification by the Aureole Model

Transition zones have been observed and measured (Table 5) in M8 concretes for three LWA families. The volume fractions c_i of the interphase verifies: $c_i = V_a \times [(a+e)^3/a^3 - 1]$, where V_a represents the real volume fraction of aggregates in concretes. This definition takes into account the increase of the interphase volume fraction with the decrease of the inclusions size [8]. The $E_i/E_m^{exp.}$ ratios are given in Table 7 according to measurements and the range of values referred in Table 6. The experimental average radius a and the measured thickness e are also mentioned in Table 7. With no experimental observations on M9 concretes, we extrapolated these results according to the hypothesis that the transition zone decreases with the W/C ratio of the matrix. This phenomenon was observed by Vivekanandam and Patnaikuni [59].

These parameter values are consistent with the values from the literature for the LWA 4/10 430 A and 4/10 520 S. On the other hand, because of its relatively high density, and therefore its low absorption capacity, LWA 4/8 750 S presents rather similar characteristics to

Table 7
ITZ characteristics for LWACs with 4/10 430 A, 4/10 520 S and 4/8 750 S aggregates.

	a (mm)	M8		M9		M10	
		e (mm)	$E_i/E_m^{exp.}$	e (mm)	$E_i/E_m^{exp.}$	e (mm)	$E_i/E_m^{exp.}$
4/10 430 A	3.7	0.04	1/2	0.02	1/2	0	1
4/10 520 S	3.6	0.02	1/2	0.01	1/2	0	1
4/8 750 S	2.8	0.1	1/6	0.05	1/4	0	1

normal weight aggregate (NWA). For M10 concretes, zero values of e correspond to the absence of ITZ mentioned in Table 5.

So, identified Young's modulus of aggregates E_a, taking into account the paste/aggregate transition zone, are shown below (Fig. 10). The three-component model can reduce the differences initially observed in Fig. 5. For a given LWAC, the identified values are more stable from a volume fraction to another. For the same LWA, the differences between the identified values are greatly reduced. This improvement is especially remarkable for concretes made of 4/8 750 S aggregates. However, current knowledge of the microstructure does not permit to separate the influence of the mortar nature and of the ITZ on the elastic properties of lightweight aggregates.

The Young's moduli of aggregates E_a, identified by the three-component model (IDA) for the M8 concretes (Fig. 10) have been used to predict the equivalent modulus E_c of all the M9 and M10 concretes [1]. The corrected predictions are presented in Fig. 11b for the 4/10 520 S LWAC. For comparison, dashed curves correspond to the simulations computed with the mean empirical values of LWAs Young's modulus (Table 2). It clearly appears that the identification procedure based on the three-component iterative homogenisation allows improving the predictions of the elastic behaviours of LWAC.

5.4. Identification by the Impregnation Model

SEM observations showed no transition zone in concretes M8 0/4 650 A and M8 4/10 550 A (Section 4). It seems that the mortar matrix impregnates the surface of these aggregates because of their thin shell and their higher water absorption coefficient. This impregnation zone is supposed to own a thickness e equal to 1% of the aggregate's average radius (0.016 mm for M8 0/4 650 A concretes and 0.043 mm for M8 4/10 550 A concretes). A part of the LWA's volume fraction c_a is included in the concentration c_i of the impregnated interphase. The remaining volume fraction of LWAs is then $c_a = V_a \times [(b-e)^3/b^3]$ and the volume fraction of interphase c_i is defined by: $c_i = V_a \times [1-(b-e)^3/b^3]$, so that the interphase's proportion increases with the decrease of the reinforcement's size [8]. For the corresponding identified Young's moduli E_a, the related thicknesses e of the impregnation zones founded with the three-component scheme are given in Table 8.

The thickness e of the interphase seems to grow with the increase of the mechanical properties of the mortar matrix. This result should be confirmed by further SEM investigations. In our experimental study, the improvement of the mechanical properties of M9 and M10 concretes is obtained by reducing the W/C ratio, while adding superplasticizer and silica fume (M10). We can have the following assumptions: the superplasticizer deflocculates the cement particles so that the cement grains remain isolated and smaller, what allows easier impregnation of the aggregates' shell in M9 and M10 concretes than in M8 concretes. Furthermore, for M10 concretes, besides the superplasticizer, silica fume, which is finer than cement, can more easily enter into the pores of the aggregates and thus induce a stronger impregnation thickness e.

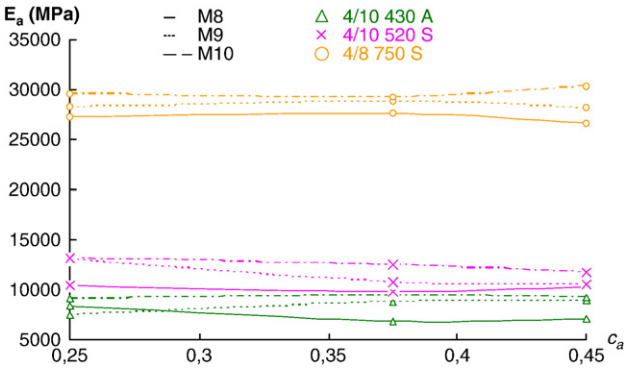

Fig. 10. LWAs Young's modulus E_a identified by the Aureole Model.

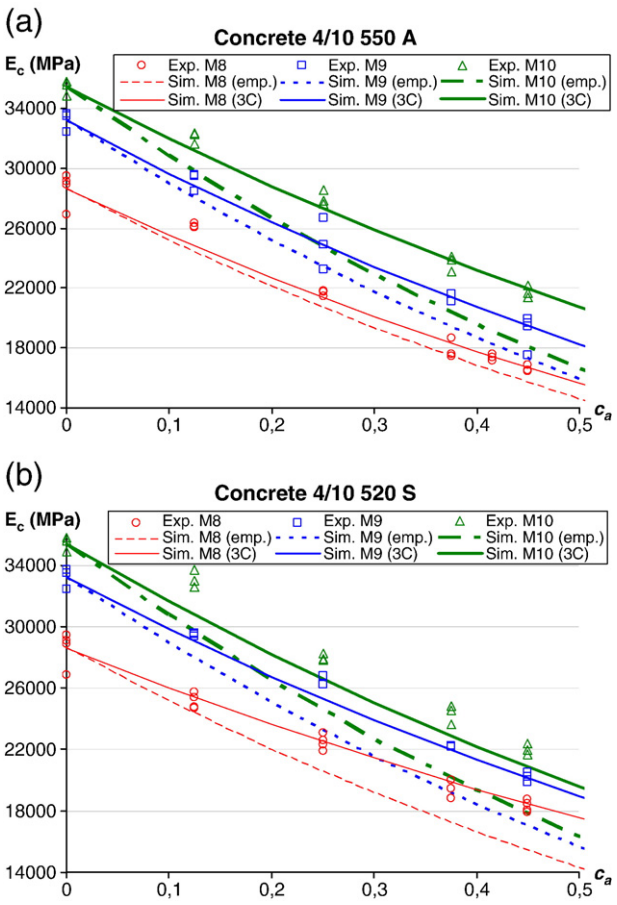

Fig. 11. Evolution of the Young's modulus of LWAC computed with the identified values E_a (Aureole or Impregnation Models). Comparison to simulations based on empirical estimations (Table 2) and to experiments: (a) concretes with 4/10 550 A aggregates; (b) concretes with 4/10 520 S aggregates.

The identified values of E_a for the aggregates 0/4 650 A (6073 MPa) and 4/10 550 A (7643 MPa) have been used to predict the equivalent Young's modulus E_c of all M9 and M10 concretes with the iterative homogenisation (IDA) based on the three-component scheme (Fig. 9) [1]. Results are plotted in Fig. 11a for the LWACs 4/10 550 A. Compared to experimental values, the identified Young's modulus of aggregates E_a can lead to good predictions of the Young's modulus of lightweight aggregate concretes.

The interpretations of the three-component scheme (Fig. 9) allow to define, for each type of lightweight aggregates, and according to the experimental observations, the best suited modelling to identify a LWA Young's modulus E_a. Fig. 11 illustrates the observed improvements for LWACs owning an interfacial transition zone (Fig. 11a) and those having a mortar impregnation zone in the aggregate's surface (Fig. 11b). Both iterative schemes allow improving significantly the computed predictions, compared to those associated to the empirical

Table 8
Thicknesses of the impregnation zone for LWACs with 0/4 650 A and 4/10 550 A aggregates.

	a (mm)	M8	M9	M10
		e (mm)	e (mm)	e (mm)
0/4 650 A	1.6	0.016	0.036	0.123
4/10 550 A	4.3	0.043	0.179	0.376

Table 9
Summary of the identified microstructural characteristics for the ITZ and the LWAs according to the adapted three-component iterative homogenisation.

LWAs		0/4 650 A	4/10 550 A	4/10 430 A	4/10 520 S	4/8 750 S
Three-component scheme		IM	IM	AM	AM	AM
Interphase thickness e (mm)	M8	0.016	0.043	0.04	0.02	0.1
	M9	0.036	0.179	0.02	0.01	0.05
	M10	0.123	0.376	0	0	0
Interphase Young's modulus E_i (MPa)	M8	28,588	28,588	14,294	14,294	4765
	M9	33,183	33,183	16,592	16,592	8296
	M10	35,397	35,397	35,397	35,397	35,397
LWA Young's modulus E_a (MPa)		6073	7643	7400–9280	10,220–12,470	27,170–29,700
Mean empirical value E_a (MPa) [28]		6870	6790	4340	6490	19,900

IM: Impregnation Model, AM: Aureole Model.

values E_a only based on the dry density of aggregates (Eq. (1)). Table 9 presents a summary of the identified values, specifies the used three-component modelling and recalls, for comparison, the empirical estimations of E_a only based on the dry volume density of lightweight aggregates. The differences between the empirical estimations and the identified values can reach a factor 2 for lightweight aggregates sensitive to the Aureole phenomena.

6. Conclusions and perspectives

The objective of the double approach (experimental and numerical) carried out in this work is to analyse and predict the mechanical performances of LWAC according to the quality of the matrix, the properties and the volume fraction of the LWA, as well as the characteristics of the matrix/aggregate interface.

Different homogenisation methods are proposed in the literature to estimate the elastic behaviour of heterogeneous materials. Their application to the prediction of LWAC behaviours can show significant disparities. Furthermore, the influence of the transition zone matrix/aggregate plays an important role on the global behaviour of concretes, a role which cannot be neglected and must be integrated into the modelling. Consequently, iterative homogenisations are proposed to accurately predict the macroscopic behaviours of LWAC, according to their specificities of component proportions, elastic moduli ratios and interfacial transition zone (ITZ) characteristics.

The observations with scanning electron microscope (SEM) show that the LWACs have a matrix/aggregate interfacial transition zone less porous and thinner than normal weight concretes (NWC). According to the W/C ratio, and depending on the shell structure of the LWA, the physicochemical processes in the interphase zone are different. When aggregates have low absorption capacity (low porosity or dense thick shell), then there exists a transition zone more porous than the matrix. This zone disappears for concretes with low W/C ratio and containing silica fume. On the other hand, for clay aggregates having high absorption capacity, it seems that an impregnation zone of the paste develops in aggregates' surface.

Iterative homogenisation provides attractive numerical tools, of easy implementation, which can be advisedly used in the identification procedures of microstructural parameters [21]. It unifies the predictions of the equivalent elastic behaviours, independently of the gap between the elastic moduli of the phases and whatever the reinforcements volume fraction. Different implementations can be indeed carried out to optimise the convergence of the iterative process and thus reduce computation time. Iterative homogenisation is supported in this work by various related developments and by new applications, especially in terms of tested materials and microstructural identifications. The enriched three-component models here proposed enable to take into account the interphase between the mortar matrix and the aggregates in the modelling of LWACs behaviours. Depending on the families of LWA and on the type of mortar matrix (normal, HP, VHP), the results of SEM observations (transition zone or paste impregnation) are integrated in the modelling in order to propose numerical tools, as for prediction as for identification, adapted to the LWACs specificities. Confrontations of the numerical predictions of equivalent LWAC behaviours to the experimental results attest to the effectiveness of the proposed three-component iterative homogenisation. Furthermore, from experimental measurements, an inverse approach allows identifying LWAs Young's modulus as well as elastic and geometric characteristics of the ITZ. In particular, iterative homogenisation provides an identification method of the Young's modulus of LWAs independent of their dry density and so allows overcoming the uncertainties inherent to the empirical relations.

A wide range of lightweight aggregate concretes has been tested. The identified microstructural parameters of LWA and ITZ lead to accurately predict the evolutions of the LWAC behaviours observed in experiments. This good agreement between experiments and models validates the proposed methodologies of homogenisation and identification. Iterative homogenisation allows also computing accurate fields of local strains and stresses. It can be then used to predict the compressive strength of LWAC according to the distributions of the micro-stresses and failure criterion of concretes [1].

Acknowledgement

The authors acknowledge the Conseil Régional of Ile-de-France for the financial support.

References

[1] Y. Ke, Caractérisation du comportement mécanique des bétons de granulats légers: expérience et modélisation, Thèse de doctorat de l'Université de Cergy-Pontoise, 2008. http://biblioweb.u-cergy.fr/theses/08CERG0395.pdf.
[2] K. Melby, E.A. Jordet, C. Hansvold, Long-span bridges in Norway constructed in high-strength LWA concrete, Eng. Struct. 18 (11) (1996) 845–849.
[3] A.K. Haug, S. Fjeld, A floating concrete platform hull made of lightweight aggregate concrete, Eng. Struct. 18 (11) (1996) 831–836.
[4] R. Zouari, A. Benhamida, H. Dumontet, A micromechanical iterative approach for the behaviour of polydispersed composites, Int. J. Solids Struct. 45 (11–12) (2008) 3139–3152.
[5] P.M. Suquet, Continuum Micromechanics, Volume 377 of CISM Course and Lecture Notes, Springer Verlag, Wien New York, 1997.
[6] J. Sanchez-Hubert, E. Sanchez-Palencia, Introduction aux méthodes asymptotiques et à l'homogénéisation: application à la mécanique des milieux continus, Masson, , 1992.
[7] A. Zaoui, Continuum micromechanics: survey, J. Eng. Mech. ASCE 128 (8) (2002) 808–816.
[8] S. Caré, Influence of aggregates on chloride diffusion coefficient into mortar, Cem. Concr. Res. 33 (7) (2003) 1021–1028.
[9] F. Grondin, H. Dumontet, A. Benhamida, G. Mounajed, H. Boussa, Multi-scales modelling for the behaviour of damaged concrete, Cem. Concr. Res. 37 (10) (2007) 1453–1462.
[10] F. De Larrard, Une approche de la formulation des bétons légers de structure, Bull. Liaison Ponts Chaussées 195 (1995) 39–47 Janvier-Février.
[11] N. Schmitt, A. Burr, Y. Berthaud, J. Poirier, Micromechanics applied to the thermal shock behavior of refractory ceramics, Mech. Mater. 34 (11) (2002) 725–747.
[12] Z. Hashin, P.J.M. Monteiro, An inverse method to determine the elastic properties of the interphase between the aggregate and the cement paste, Cem. Concr. Res. 32 (8) (2002) 1291–1300.
[13] O. Bernard, F.J. Ulm, E. Lemarchand, A multiscale micromechanics-hydration model for the early-age elastic properties of cement-based materials, Cem. Concr. Res. 33 (9) (2003) 1293–1309.
[14] J. Sanahuja, L. Dormieux, G. Chanvillard, Modelling elasticity of a hydrating cement paste, Cem. Concr. Res. 37 (10) (2007) 1427–1439.

[15] S. Nemat-Nasser, M. Hori, Micromechanics: Overall Properties of Heterogeneous Materials, North-Holland, Amsterdam, London, New York, Tokyo, 1993.
[16] A. Zaoui, Matériaux hétérogènes et composites [Heterogeneous materials and composites], Lecture Notes, École Polytechnique, Palaiseau, France, 1997, In French.
[17] Z. Hashin, Analysis of composite material: a survey, J. Appl. Mech. 50 (1983) 481–505.
[18] Z. Hashin, The elastic moduli of heterogeneous materials, J. Appl. Mech. 29 (1962) 143–150.
[19] T. Mori, K. Tanaka, Average stress in matrix and average elastic energy of materials with misfitting inclusions, Acta Metall. 21 (5) (1973) 571–574.
[20] Y. Benveniste, A new approach to the application of Mori–Tanaka's theory in composite materials, Mech. Mater. 6 (2) (1987) 147–157.
[21] Y. Ke, S. Ortola, A.L. Beaucour, R. Cabrillac, H. Dumontet, Influence of aggregates on mechanical behavior of lightweight aggregate concrete: experimental characterization and modelling, First Euro Mediterranean in Advances on Geomaterials and Structures, Hammamet, Tunisia, 2006.
[22] M. Haboussi, H. Dumontet, J.L. Billoët, On the modelling of interfacial transition behavior in composite materials, Comput. Mater. Sci. 20 (2) (2001) 251–266.
[23] G. Ramesh, E.D. Sotelino, W.F. Chen, Effect of transition zone on elastic moduli of concrete materials, Cem. Concr. Res. 26 (4) (1996) 611–622.
[24] K.M. Lee, J.H. Park, A numerical model for elastic modulus of concrete considering ITZ, Cem. Concr. Res. 38 (2008) 396–402.
[25] Y. Ke, A.L. Beaucour, S. Ortola, H. Dumontet, R. Cabrillac, Influence of volume fraction and characteristics of lightweight aggregate concrete on the mechanical properties of concrete, Constr. Build. Mater. 23 (8) (2009) 2821–2828.
[26] J.M. Torrenti, P. Dentec, C. Boulay, J.F. Sembla, Projet de processus d'essai pour la détermination du module de déformation longitudinale du béton, Bull. Lab. Ponts Chaussées 220 (1999) 79–81.
[27] Y. Ke, Influence des paramètres de formulation sur les performances mécaniques des bétons légers: étude expérimentale et modélisation, 26èmes Rencontres AUGC2008, Nancy, France, 2008.
[28] M. Arnould, M. Virlogeux, Granulats et bétons légers, Presses des Ponts et Chaussées, 1986, ISBN 2-85978-086-6.
[29] J.D. Eshelby, The determination of the elastic field of an ellipsoidal inclusion, and related problems, Proceedings of the Royal Society of London, 1957, pp. 376–396.
[30] B. Budiansky, On the elastic moduli of some heterogeneous materials, J. Mech. Phys. Solids 13 (4) (1965) 223–227.
[31] G.J. Weng, Some elastic properties of reinforced solids, with special reference to isotropic ones containing spherical inclusion, Int. J. Eng. Sci. 22 (1984) 845–856.
[32] J. Aboudi, Mechanics of Composite Materials, Elsevier, 1991.
[33] S. Torquato, Random Heterogeneous Materials, Springer, Berlin, 2002.
[34] F. Devries, H. Dumontet, G. Duvaut, F. Léné, Homogenization and damage for composites materials, Int J Numer Meth Eng 27 (1989) 285–298.
[35] F. Bouchelaghem, A. Benhamida, H. Dumontet, Mechanical damage behaviour of an injected sand by periodic homogenization method, Comp. Mater. Sci. 38 (2007) 473–481.
[36] M. Bornert, T. Bretheau, P. Gilormini, Homogénéisation en mécanique des matériaux 1, Matériaux aléatoires élastiques et milieu périodiques, Collection Mécanique et Ingénierie des Matériaux, Hermes Sciences Publications, Paris, 2001.
[37] U. Prahl, S. Bourgeois, T. Pandorf, M. Aboutayeb, O. Debordes, D. Weichert, Damage parameter identification by a periodic homogenization approach, Comp. Mater. Sci. 25 (1–2) (2002) 159–165.
[38] E. Hervé, A. Zaoui, N-layered inclusion-based micromechanical modelling, Int. J. Eng. Sci. 31 (1) (1993) 1–10.
[39] M. Bornert, C. Stolz, A. Zaoui, Morphologically representative pattern-based bounding in elasticity, J. Mech. Phys. Solids 44 (1996) 307–331.
[40] L. Dormieux, F.J. Ulm, Applied Micromechanics of Porous Media, Volume 480 of CISM Course and Lecture Notes, Springer, Wien New York, 2005.
[41] L. Dormieux, D. Kondo, F.J. Ulm, Microporomechanics, John Wiley & Sons, 2006.
[42] F.J. Ulm, G. Constantinides, F.H. Heukamp, Is concrete a poromechanics material? — a multiscale investigation of poroelastic properties, Mater. Struct. Mater. Construct. 37 (1) (2004) 43–58.
[43] V. Smilauer, Z. Bittnar, Microstructure-based micromechanical prediction of elastic properties in hydrating cement paste, Cem. Concr. Res. 36 (9) (2006) 1708–1718.
[44] B. Pichler, S. Scheiner, Ch. Hellmich, From micron-sized needle-shaped hydrates to meter-sized shotcrete tunnel shells: micromechanical upscaling of stiffness and strength of hydrating shotcrete, Acta Geotech. 3 (4) (2008) 273–294.
[45] Z. Hashin, S. Shtrikman, A variation approach to the theory of the elastic behavior of multiphase materials, J. Mech. Phys. Solids 11 (2) (1963) 127–140.
[46] F. De Larrard, R. Le Roy, Relation entre formulation et quelques propriétés mécaniques des bétons à hautes performances, Mater. Struct. 25 (1992) 464–475.
[47] A. Benhamida, H. Dumontet, Étude micromécanique du comportement de matériaux hétérogènes par une approche itérative, in: Hermes (Ed.), Proceedings of 6th Colloque National en Calcul des Structures, Giens, France, 2003, pp. 523–530.
[48] A. Brini, F. Pradel, A. Benhamida, H. Dumontet, Aging damage of immersed syntactic foams under coupled effects of pressure and aqueous corrosion, Proceedings of Fourteenth International Conference on Composite Materials, San Diego, USA, July 2003.
[49] S. Smaoui, A. Benhamida, I. Djeran-Maigre, H. Dumontet, Micro-macro approaches coupled to iterative process for non linear porous media, Comput. Mater. Contin. 3 (4) (2006) 153–162.
[50] M.A. Tasdemir, C. Tasdemir, S. Akyüz, A.D. Jefferson, F.D. Lydon, B.I.G. Barr, Evaluation of strains at peak stresses in concrete: a three-phase composite model approach, Cem Concr. Comp. 20 (4) (1998) 301–318.
[51] C.C. Yang, R. Huang, A two phase model predicting the compressive strength of concrete, Cem. Concr. Res. 26 (10) (1996) 1567–1577.
[52] A. Nilsen, P.J.M. Monteiro, O.E. Gjorv, Quality assessment of lightweight aggregate, Cem. Concr. Res. 24 (8) (1994) 1423–1427.
[53] T.Y. Lo, H.Z. Cui, Effect of porous lightweight aggregate on strength of concrete, Mater. Lett. 58 (6) (2004) 916–919.
[54] M.H. Zhang, O.E. Gjorv, Microstructure of the interfacial zone between lightweight aggregate and cement paste, Cem. Concr. Res. 20 (4) (1990) 610–618.
[55] A. Elsharief, M.D. Cohen, J. Olek, Influence of lightweight aggregate on the microstructure and durability of mortar, Cem. Concr. Res. 35 (7) (2005) 1368–1376.
[56] J.M. Berthelot, Matériaux composites, comportement mécanique et analyses des structures, Masson, Paris, 1996.
[57] T. Mura, Micromechanics of Defects in Solids, Martinus Nijhoff Publishers, 1982, pp. 67–71.
[58] R.M. Christensen, K.H. LO, Solution for effective shear properties in three phase sphere and cylinder models, J. Mech. Phys. Solids 27 (1979) 315–330.
[59] K. Vivekanandam, I. Patnaikuni, Transition zone in high performance concrete during hydration, Cem. Concr. Res. 27 (6) (1997) 817–823.